

Intelligent Hybrid Vehicle Power Control- Part II: Online Intelligent Energy Management

Yi L. Murphey¹, *Senior Member, IEEE*, Jungme Park¹, Leonidas Kiliaris¹, Ming Kuang², *Member, IEEE*, Abul Masrur³, *Fellow, IEEE*, Anthony Phillips², Qing Wang², *Member IEEE*

¹Department of Electrical and Computer Engineering, University of Michigan-Dearborn
(Phone: 313-593-5028, Fax: 313-583-6336, Email: yilu@umich.edu)

²Ford Motor Company, Dearborn, MI, USA.

³The US Army RDECOM-TARDEC, Warren, MI 49307.

Abstract— This is the second paper in a series of two that describe our research in intelligent energy management in a hybrid electric vehicle (HEV). Energy management in Hybrid Electric Vehicles (HEV) has been actively studied recently because of its potential to significantly improve fuel economy and emission control. Because of the dual-power-source nature and the complex configuration and operation modes in a HEV, energy management is more complicated and important than in a conventional vehicle. Most of the existing vehicle energy optimization approaches do not incorporate knowledge about driving patterns into their vehicle energy management strategies. Our approach is to use machine learning technology combined with roadway type and traffic congestion level specific optimization to achieve quasi-optimal energy management in hybrid vehicles.

In this series of two papers, we present a machine learning framework that combines Dynamic Programming with neural networks to learn about roadway type and traffic congestion level specific energy optimization, and an integrated online intelligent energy controller to achieve quasi-optimal power management in hybrid vehicles. In the first paper we presented a machine learning framework, *ML_EMO_HEV*, developed for learning the knowledge about energy optimization in an HEV. The framework consists of machine learning algorithms for predicting driving environments and for generating optimal power split of the HEV system for a given driving environment. Experiments are conducted to evaluate these algorithms using a simulated Ford Escape Hybrid vehicle model provided in PSAT (Powertrain Systems Analysis Toolkit).

In this second paper, we present three online intelligent energy controllers, *IEC_HEV_SISE*, *IEC_HEV_MISE*, and *IEC_HEV_MIME*. All three online intelligent energy controllers were trained within the machine learning framework, *ML_EMO_HEV* were trained to generate the best combination of engine power and battery power in real-time such that the total fuel consumption over whole driving cycle is minimized while still meeting the driver's demand and the system constraints including engine, motor, battery, and generator operation limits. The three online controllers were integrated into the Ford Escape Hybrid vehicle model for online performance evaluation. Based on their performances on 10 test drive cycles provided by the PSAT library, we can conclude that the roadway type and traffic congestion level specific machine learning of optimal energy management is effective for in-vehicle energy

Report Documentation Page

Form Approved
OMB No. 0704-0188

Public reporting burden for the collection of information is estimated to average 1 hour per response, including the time for reviewing instructions, searching existing data sources, gathering and maintaining the data needed, and completing and reviewing the collection of information. Send comments regarding this burden estimate or any other aspect of this collection of information, including suggestions for reducing this burden, to Washington Headquarters Services, Directorate for Information Operations and Reports, 1215 Jefferson Davis Highway, Suite 1204, Arlington VA 22202-4302. Respondents should be aware that notwithstanding any other provision of law, no person shall be subject to a penalty for failing to comply with a collection of information if it does not display a currently valid OMB control number.

1. REPORT DATE

30 JUN 2012

2. REPORT TYPE

Journal Article

3. DATES COVERED

30-06-2012 to 30-06-2012

4. TITLE AND SUBTITLE

Intelligent Hybrid Vehicle Power Control- Part II: Online Intelligent Energy Management

5a. CONTRACT NUMBER

5b. GRANT NUMBER

5c. PROGRAM ELEMENT NUMBER

6. AUTHOR(S)

Abul Masrur; Yi. Murphey; Jungme Park; Ming Kuang

5d. PROJECT NUMBER

5e. TASK NUMBER

5f. WORK UNIT NUMBER

7. PERFORMING ORGANIZATION NAME(S) AND ADDRESS(ES)

University of Michigan - Dearborn, Department of Electrical and Computer Engineering, Dearborn, MI, 48128

8. PERFORMING ORGANIZATION REPORT NUMBER

; #23019

9. SPONSORING/MONITORING AGENCY NAME(S) AND ADDRESS(ES)

U.S. Army TARDEC, 6501 E.11 Mile Rd, Warren, MI, 48397-5000

10. SPONSOR/MONITOR'S ACRONYM(S)

TARDEC

11. SPONSOR/MONITOR'S REPORT NUMBER(S)

#23019

12. DISTRIBUTION/AVAILABILITY STATEMENT

Approved for public release; distribution unlimited

13. SUPPLEMENTARY NOTES

Paper submitted to IEEE Transactions on Vehicular Technology

14. ABSTRACT

This is the second paper in a series of two that describe our research in intelligent energy management in a hybrid electric vehicle (HEV). Energy management in Hybrid Electric Vehicles (HEV) has been actively studied recently because of its potential to significantly improve fuel economy and emission control. Because of the dual-power-source nature and the complex configuration and operation modes in a HEV, energy management is more complicated and important than in a conventional vehicle. Most of the existing vehicle energy optimization approaches do not incorporate knowledge about driving patterns into their vehicle energy management strategies. Our approach is to use machine learning technology combined with roadway type and traffic congestion level specific optimization to achieve quasi-optimal energy management in hybrid vehicles. In this series of two papers, we present a machine learning framework that combines Dynamic Programming with neural networks to learn about roadway type and traffic congestion level specific energy optimization, and an integrated online intelligent energy controller to achieve quasi-optimal power management in hybrid vehicles. In the first paper we presented a machine learning framework, ML_EMO_HEV, developed for learning the knowledge about energy optimization in an HEV. The framework consists of machine learning algorithms for predicting driving environments and for generating optimal power split of the HEV system for a given driving environment. Experiments are conducted to evaluate these algorithms using a simulated Ford Escape Hybrid vehicle model provided in PSAT (Powertrain Systems Analysis Toolkit). In this second paper, we present three online intelligent energy controllers, IEC_HEV_SISE, IEC_HEV_MISE, and IEC_HEV_MIME. All three online intelligent energy controllers were trained within the machine learning framework, ML_EMO_HEV were trained to generate the best combination of engine power and battery power in real-time such that the total fuel consumption over whole driving cycle is minimized while still meeting the driver's demand and the system constraints including engine, motor, battery, and generator operation limits. The three online controllers were integrated into the Ford Escape Hybrid vehicle model for online performance evaluation. Based on their performances on 10 test drive cycles provided by the PSAT library, we can conclude that the roadway type and traffic congestion level specific machine learning of optimal energy management is effective for in-vehicle energy. The best controller, IEC_HEV_MISE, trained with the optimal power split generated by the DP optimization algorithm with multiple initial SOC points and single ending point can provide fuel saving range from 5% through 19%.

15. SUBJECT TERMS

Fuel economy, machine learning, energy optimization, HEV power management

16. SECURITY CLASSIFICATION OF:

a. REPORT unclassified	b. ABSTRACT unclassified	c. THIS PAGE unclassified
----------------------------------	------------------------------------	-------------------------------------

17. LIMITATION OF ABSTRACT

Same as Report (SAR)

18. NUMBER OF PAGES

22

19a. NAME OF RESPONSIBLE PERSON

control. The best controller, IEC_HEV_MISE, trained with the optimal power split generated by the DP optimization algorithm with multiple initial SOC points and single ending point can provide fuel saving range from 5% through 19%.

In conclusion, together these two papers cover the innovative technologies for modeling power flow, mathematical background of optimization in energy management, and machine learning algorithms for generating intelligent energy controllers for quasi-optimal energy flow in a power split HEV.

Index Terms— Fuel economy, machine learning, energy optimization, HEV power management

I. INTRODUCTION

Power management in Hybrid Electric Vehicles (HEV) has been actively studied recently because of its potential to significantly improve fuel economy and emission control [1-10]. Because of the dual-power-source nature and the complex configuration and operation modes in an HEV, power management is more complicated but also more important than in a conventional vehicle. Most of the existing vehicle power optimization approaches do not incorporate knowledge about driving patterns into their vehicle power management strategies. Our approach is to use machine learning technology combined with energy optimization specific to Sierra Facility Specific drive cycles [11-15] to achieve quasi-optimal power management in hybrid vehicles. The 11 standard Sierra Facility Specific drive cycles are referred as roadway types and traffic congestion levels. In a series of two papers, we present a machine learning framework that combines Dynamic Programming [8-10] with machine learning to learn about roadway type and traffic congestion level specific energy optimization, and an integrated online intelligent energy controller to achieve quasi-optimal power management in hybrid vehicles. In the first paper, we presented the machine learning architecture of the intelligent vehicle power management system, ML_EMO_HEV. This framework consists of two parts. First it contains neural learning algorithms for predicting roadway types and traffic congestion levels and driving trends based on the vehicle's recent driving history. Second, it contains roadway type and traffic congestion level specific machine learning algorithms for the purpose of optimizing the power split between the propulsion system components within the HEV. This second set of machine learning algorithms are trained using optimal solutions from offline Dynamic Programming analysis of roadway type and traffic congestion level.

In this second paper, we present an online intelligent energy controller (IEC) for HEV, IEC_HEV. IEC_HEV is developed under the ML_EMO_HEV framework, and trained by the machine learning algorithms presented in the first paper of this series. We will also cover the critical issues related to the integration of IEC_HEV to a vehicle control system, and system performance analysis on various drive cycles using different settings of learning parameters. The experiments were conducted with four different IEC_HEV models that were implemented inside PSAT.

The organization of the remainder of the paper is as follows. Section II introduces energy dynamics in a power-split HEV model. Section III presents an intelligent online energy controller, IEC_HEV, and the online implementation of IEC_HEV in a power-split HEV model. Section IV performs experiments to evaluate different versions of IEC_HEV with various cycles provided in PSAT. Section V concludes this paper.

II. ENERGY DYNAMICS IN A POWER SPLIT HEV MODEL

A power split HEV has two power sources that are connected to the driveline using a planetary gear set as shown in Figure 1. The power train consists of the engine, generator, motor, battery and planetary gear set. The planetary gear set is the key device in the power split HEV power train that connects the engine, generator, and motor as a power split device. The engine is connected to the carrier gear, the generator is connected to the sun gear and the motor is linked to the ring gear of the planetary gear set. The planetary gear set transmits power between the engine, motor, generator and front wheels. The vehicle can be propelled by either one or both of two power sources. The first power source is the combined engine and generator. This combination can be used to provide mechanical power to the driveline directly or to provide electrical power to the high voltage system. The second propulsion system consists of the motor, possibly in combination with generator. The motor (and potentially generator) can be used to propel the vehicle by drawing electrical energy from the battery or by using the high voltage energy produced by the combined engine and generator.

Because of the kinematic properties of the planetary gear set, the engine speed can be decoupled from the vehicle speed, which provides a great potential for optimizing engine efficiency [16-17]. The decoupled engine speed and the amount of battery power that is charged or discharged are the two degrees of freedom used by IEC_HEV for vehicle energy optimization. IEC_HEV, the

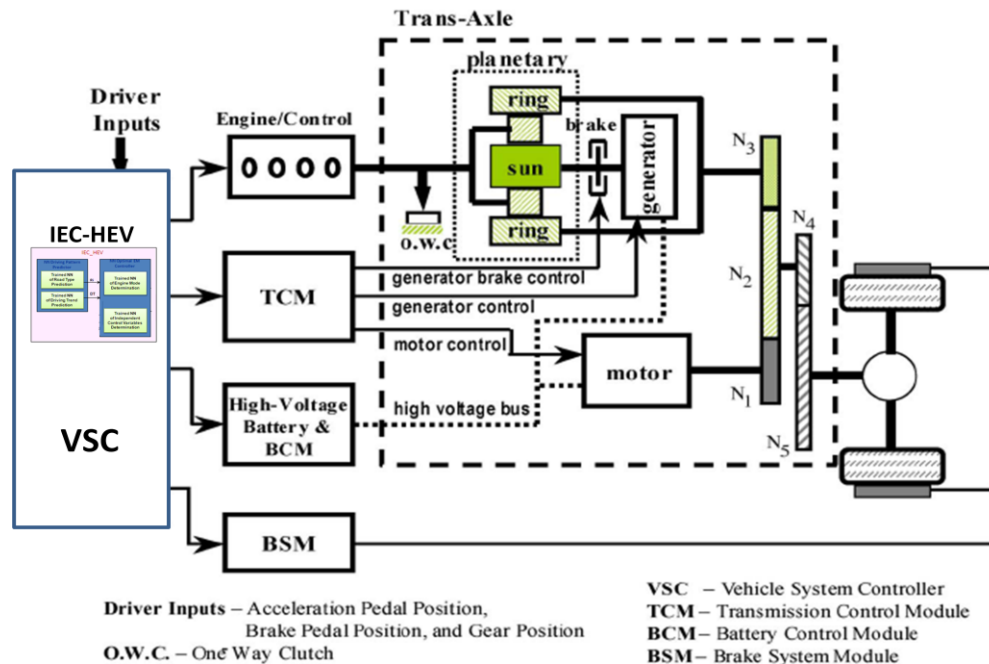


Figure 1. Power Split HEV configuration into VSC

online energy control is a component in the Vehicle System Controller (VSC). The VSC for this configuration must manage the powertrain control in order to maintain a proper level of charge in the battery. However, since two power sources are available to propel the vehicle, the VSC in this configuration has the additional responsibility of coordinating the two power sources to properly deliver power to the wheel [18]. Based on the optimal engine speed and battery power generated by the IEC_HEV, the VSC derives the speed and power of the other components (engine, motor, and generator) based on the following kinematics and dynamics of the power-split HEV system [17-19].

The kinematics of a planetary gear set defines the speed relationship between the carrier, $\omega_{carrier}$, sun gear, ω_{sun} and ring gear, ω_{ring} as shown in the equation below [19]:

$$\omega_{carrier} = \frac{N_{sun}}{N_{ring} + N_{sun}} \omega_{sun} + \frac{N_{ring}}{N_{ring} + N_{sun}} \omega_{ring} \quad (1)$$

where N_{sun} is the number of teeth of sun gear and N_{ring} is the number of teeth of ring gear. The fixed torque split between the carrier, $\tau_{carrier}$, sun gear, τ_{sun} and ring gear, τ_{ring} is defined as below:

$$\tau_{sun} = \frac{N_{sun}}{N_{ring} + N_{sun}} \tau_{carrier}, \quad \tau_{ring} = \frac{N_{ring}}{N_{ring} + N_{sun}} \tau_{carrier} \quad (2)$$

Because the planetary gear set acts as a power split device, the total of the powers of the elements in the device sum to zero. The following equations are derived based on the power flow illustrated in Figure 2.

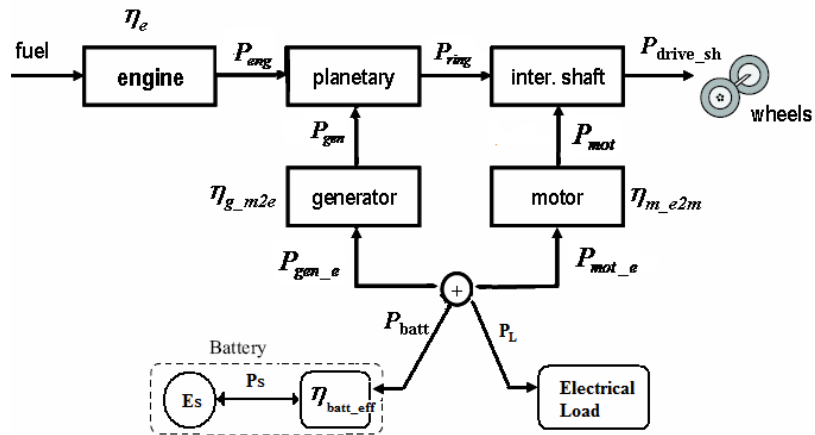


Figure 2. Power flow in a Split HEV configuration with arrows indicating positive power.

The relationship between the power delivered at the carrier, $P_{carrier}$, the power at the ring gear, P_{ring} , and the power at the sun gear, P_{sun} is described in the equation below:

$$P_{carrier} + P_{sun} + P_{ring} = 0 \quad . \quad (3)$$

In addition, the power across the electrical power net can be expressed as follows:

$$P_{batt} = -(P_{gen_e} + P_{mot_e} + P_L) = -(P_{gen} + P_{gen_loss} + P_{mot} + P_{mot_loss} + P_L) \quad (4)$$

where P_{batt} is power output at the battery terminal, P_{gen_e} is the electrical power at the generator, P_{gen_loss} is the generator power loss during power conversion using the generator efficiency, η_g , P_{mot_e} is the electrical power at the motor, P_{mot_loss} is the motor power loss during power conversion using the motor efficiency, η_m , and P_L represents the power of the electrical load. Based on equation (4) and the fact that the power at the final drive is provided by the ring gear power and motor power, equation (5) shows how the engine power, P_{eng} is represented using the power split dynamics:

$$\begin{aligned} P_{eng} &= P_{ring} + (-P_{gen}) = P_{ring} - P_{gen_e} + P_{gen_loss} = P_{ring} + P_{batt} + P_L + P_{mot_e} + P_{gen_loss} \\ &= P_{ring} + P_{batt} + P_L + P_{mot} + P_{mot_loss} + P_{gen_loss} = P_{drive_sh} + P_{batt} + P_L + P_{mot_loss} + P_{gen_loss} \end{aligned} \quad (5)$$

The ring gear speed, ω_{ring} , and the motor speed, ω_{motor} , are coupled to the driveshaft speed, $\omega_{drive-sh}$, and correspondingly, the vehicle speed, v_s . Based on this constraint, from the quasi-optimal engine speed $\omega_{eng} = (\omega_{carrier})$ generated by the IEC-HEV, the VSC derives the sun gear speed, ω_{sun} . The quasi-optimal battery power, P_{batt} , generated by IEC_HEV is used by VSC to determine the quasi-optimal motor torque and power. Thus a quasi-optimal power split is achieved.

III. INTELLIGENT ONLINE ENERGY CONTROL

In general HEV operations, the engine can be operated in three states as illustrated in Figure 3: “engine off”, “engine start-up”, and “engine on.” When the engine is in the “off” state, it goes to the “start-up” state when the driver’s power demand is bigger than a threshold. The threshold value is typically calculated based on the current battery state of charge, SOC. Figure 4 shows such a threshold function for the Ford Escape provided in the PSAT modeling environment. Once the engine speed is higher than the engine idle speed (e.g. 83.76 rad/sec) then the engine goes to the ‘engine-on’ state, and stays there until the driver’s power demand becomes negative. Then the engine is turned off, i.e. it enters the “engine off” state from "engine on" state. The Intelligent Energy Controller for HEV, IEC_HEV, is only operational during the "engine on" state. The conditions used in Figure 3 to illustrate the state transitions were derived from the Ford Escape HEV model provided by PSAT library.

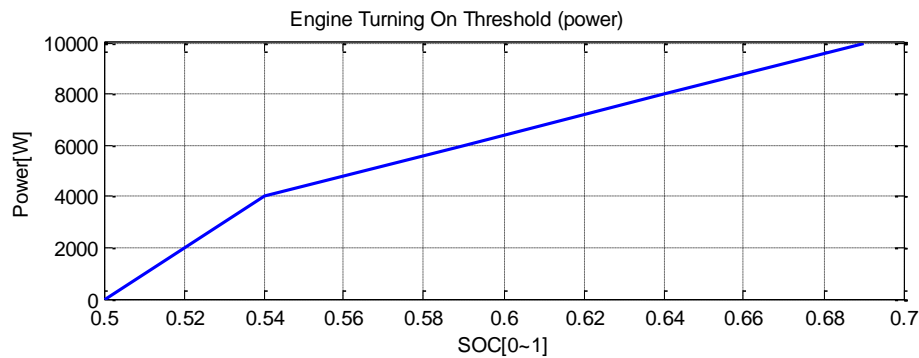
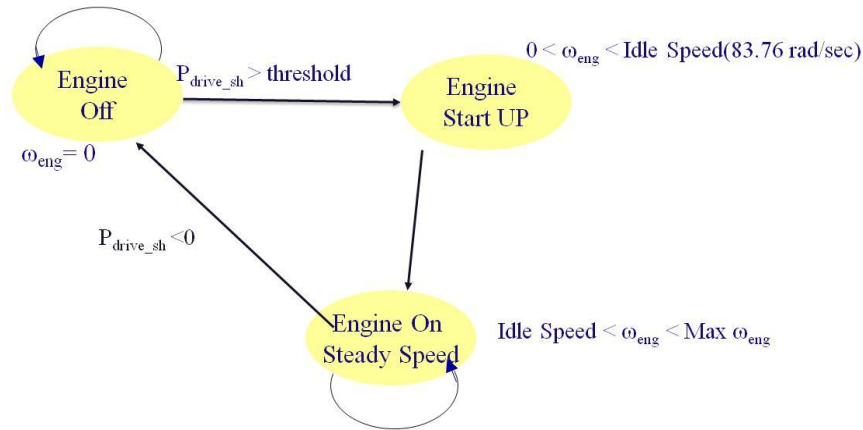


Figure 4. Threshold of driver power demand as a function of SOC for engine turning on.

When the engine is in the “on” state, the power split between the mechanical and the electrical path at every time instance determines the fuel economy over the entire drive cycle. IEC-HEV is designed and trained to generate, at every time instance, an intelligent power split between the two energy sources, mechanical power from the engine and the electrical power from the battery, so the fuel consumption over the entire drive cycle is optimized and, at the same time, the driver’s demand and the system constraints (engine, motor, battery, and generator limits) are fully met. Because global optimization algorithms such as Dynamic Programming require the knowledge about the entire drive cycle being known a priori, therefore these methods are not directly applicable to on-line implementation since the future driving information is generally unknown during vehicle operations [19-21].

Our approach is to use machine learning technology to predict the short term driving environment, i.e. roadway type and traffic congestion level and driving trend, and apply the appropriate energy split in the real time operation of a drive cycle. We presented, in Part I of this paper series, the machine learning algorithms for training neural networks to emulate the optimal power control of an HEV generated by DP, and the neural networks to predict driving environment, which includes roadway type and traffic

congestion level the vehicle is currently on and the driving trend of the vehicle. IEC-HEV is an integrated system of these neural networks. Figure 5 illustrates the major components in the intelligent energy controller IEC-HEV. IEC_HEV consist of three types of neural networks: NN_RT&TC, a neural network trained to predict roadway type and traffic congestion level based on the vehicle dynamics, NN_DT, a neural network trained to predict driving trend, and the $2K$ power split neural networks for K standard roadway types and traffic congestion levels. As discussed in the first paper of the series, we use in this research the 11 Sierra FS drive cycles as the standard description of roadway types and traffic congestion levels. Therefore we have $K = 11$. For the convenience of description we denote the 11 standard roadway types and traffic congestion levels as $R_i, i=1, \dots, 11$. For each roadway type and traffic congestion level R_i , two neural networks have been developed and trained, $NN_{P_{bat}}^i$ to predict the optimal battery power P_{batt} , and $NN_{\omega_{eng}}^i$ to predict the optimal engine speed ω_{eng} . The training details of all these neural networks are presented in the Part I of this paper series. The output from the power split neural networks are used to generate the optimal engine power, $P_{eng}(t)$ following the equation (1)~(5). Both the engine power $P_{eng}(t)$ and the engine speed $\omega_{eng}(t)$ are being checked to make sure they are within the constraints such as being less than the maximum engine power and the maximum engine speed. Therefore the desired engine power and engine speed are generated.

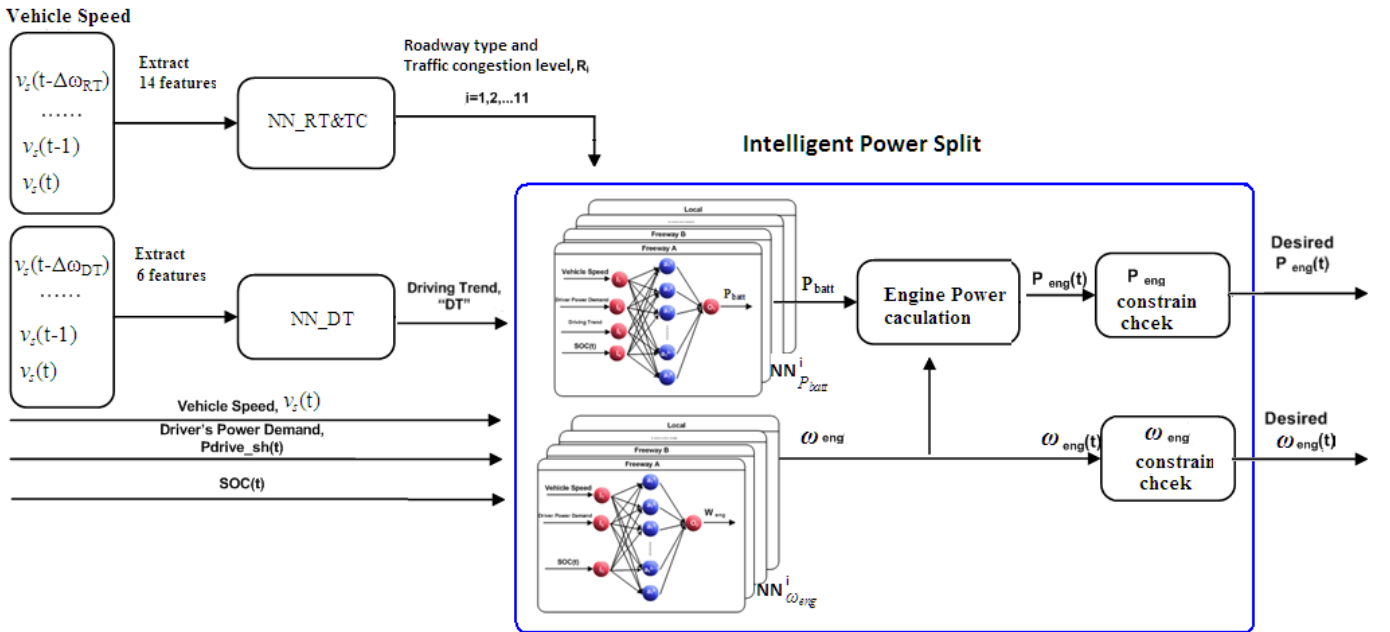


Figure 5. Computational flow in IEC-HEV during the power split mode at every time instance t .

During online driving, at the beginning of a drive cycle ($t < \Delta W_{RT}$), IEC-HEV uses a power split strategy provided by the default Ford Escape power control in PSAT. When $t \geq \Delta W_{RT}$, at every time instance $t = \Delta W_{RT} + j \cdot \Delta t$, $j = 0, \dots$, until the end of the drive cycle, where Δt is very small, e.g. 1 second, IEC-HEV obtains the current vehicle state, represented as $V_state(t) = \{v_s(t), P_{drive_sh}(t), SOC(t)\}$ where $v_s(t)$ is the vehicle speed, $P_{drive_sh}(t)$ is the driver's power demand, $SOC(t)$ is the state of charge of the battery, uses the data combined with the vehicle speed data from last a few seconds to generate the desired engine power and engine speed. The IEC-HEV has the following major computational steps. First it calls the neural network NN_RT&TC to predict the current roadway type and traffic congestion level, and the neural network NN_DT to predict the driving trend.

NN_RT&TC makes the prediction based on the fourteen features extracted from the vehicle speed profile during time interval $[t - \Delta W_{RT}, t]$, where ΔW_{RT} is the window size, which was discussed extensively in [22]. They are distance traveled within this time interval, the maximum speed, acceleration and deceleration, average speed, acceleration and deceleration, standard deviation of acceleration, % of time the vehicle traveled within speed 15 ~ 30km/h, % of time within speed > 110km/h, % of time in deceleration within interval $-10 \sim -2.5\text{m/s}^2$, % of time in deceleration within intervals $-10 \sim -2.5\text{m/s}^2$, $-2.5 \sim -1.5\text{m/s}^2$, and $-1.5 \sim -1\text{m/s}^2$, and the number of acceleration shifts within this time interval. The output of NN_RT&TC is R_i , the roadway type and traffic congestion level predicted at time t , one of the 11 standard Sierra FS drive cycles, $i=1, \dots, 11$.

The neural network, NN_DT, was developed and trained to predict the current driving trend represented in one of five states, no-speed, low speed cruise, high speed cruise, acceleration, and deceleration. The driving trend reflects the driver's reaction to the traffic condition, therefore is an important factor that affects fuel consumption. The input to NN_DT are six features calculated from the past vehicle speed profile within the time interval $[t - \Delta W_{DT}, t)$. They are, the average speed, maximum speed, minimum speed and average acceleration, during the time period $[t - \Delta W_{DT}, t)$, the vehicle speed at $(t - \Delta W_{DT})$, and the vehicle speed at t .

Since driving trend can change in very short time interval, a small window size should be used here. In our system we used $\Delta W_{dt} = 9$ seconds. The design and training details of these neural networks were presented in [22]. Based on the roadway type and traffic congestion level R_i predicted by the neural network NN_RT&TC, IEC-HEV calls the two neural networks, $NN_{P_{bat}}^i$ and $NN_{\omega_{eng}}^i$, which were trained for generating optimal battery power, $P_{bat}(t)$, and engine speed $\omega_{eng}(t)$ respectively for the roadway type and traffic congestion level R_i . The input variables to $NN_{P_{bat}}^i$ are $\{v_s(t), P_{drive_sh}(t), SOC(t), DT(t)\}$, where $v_s(t)$ is the vehicle speed, $P_{drive_sh}(t)$ is the driver's power demand, $DT(t)$ is the driving trend, $SOC(t)$ is the state of charge of the battery. The input variables to $NN_{\omega_{eng}}^i$, are $\{v_s(t), P_{drive_sh}(t), SOC(t)\}$. Based on the desired battery power $P_{bat}(t)$, and engine $\omega_{eng}(t)$, we calculate the following vehicle parameters can be calculated, motor power $P_{mot}(t)$, motor power loss $P_{mot_loss}(t)$, generator power $P_{gen}(t)$, and generator

power loss, $P_{gen_loss}(t)$, as explained in equations(6)-(10) in [22]. Then the desired engine power $P_{eng}(t)$ can be obtained by using the following equation:

$$P_{eng}(t) = P_{drive_sh}(t) + P_{batt}(t) + P_{mot_loss}(t) + P_{gen_loss}(t) + P_L. \quad (6)$$

IV. SYSTEM IMPLEMENTATION AND EVALUATIONS

The intelligent energy controller, IEC-HEV has been fully implemented on the Ford Escape model provided in the PSAT library. The major components and parameters of the power split system of the Ford Escape model are listed in Table I. Figure 6 shows integrated IEC_HEV in the vehicle propelling system of the Ford Escape model. IEC_HEV is placed between the Driver Model and the subsystem control. The desired battery power and engine speed generated by the neural networks are used to generate torques and speeds in a engine, a generator and a motor following the equations given in the Part I of this series [22].

TABLE I
MAJOR COMPONENTS OF THE POWER SPLIT SYSTEM IN THE FORD ESCAPE MODEL PROVIDED BY PSAT

Components	Description
Engine	<ul style="list-style-type: none"> Ford Escape Hybrid MY05 gasoline engine 2.3L 99kW
Planetary Gear Set and Driveline	<ul style="list-style-type: none"> $N_{ring} = 79$ $N_{sun} = 33$, Wheel Radius = 0.348m, Final Drive Ratio = 3.77
Generator	<ul style="list-style-type: none"> Ford Escape Hybrid MY05 permanent magnet motor Continuous Power = 17kW, Peak Power = 33kW
Motor	<ul style="list-style-type: none"> Ford Escape Hybrid MY05 permanent magnet motor Continuous Power = 33kW Peak Power = 65kW
Battery	<ul style="list-style-type: none"> Toyota Prius MY04 Battery (ess_nimh_6_168_panasonic_MY04_Prius) Capacity = 6.5Ah, Cell number = 168

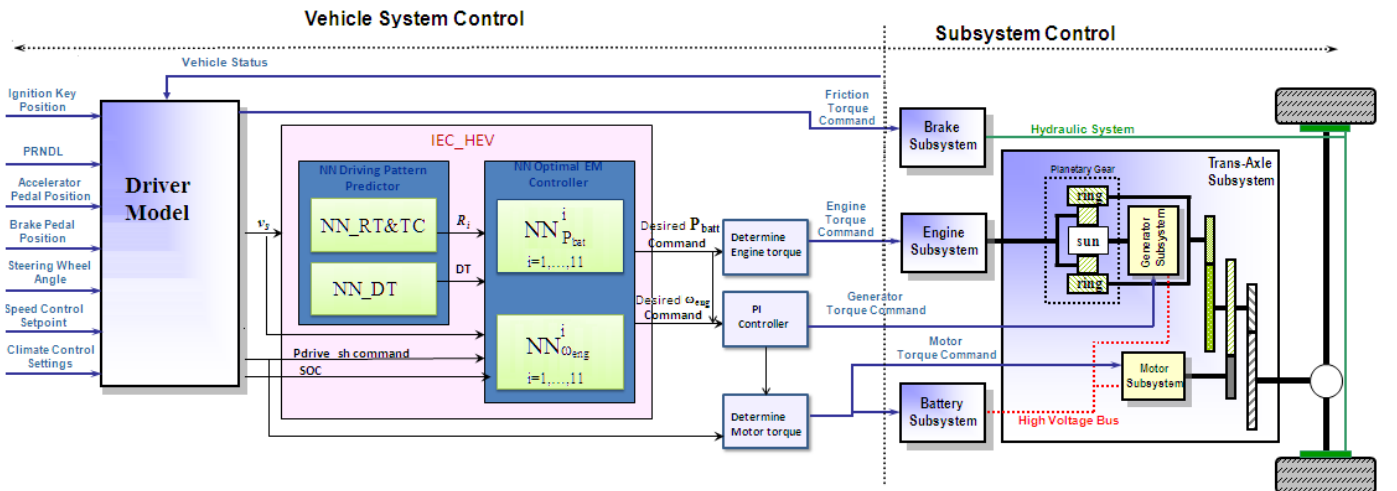


Figure 6. Implementation of IEC-HEV in the Ford Escape model provided by PSAT

In order to conduct an in-depth study on the effectiveness of the proposed machine learning framework ML_EMO_HEV, we implemented four different versions of the machine learning algorithm for optimal power split, *IEC_HEV_SISE*, *IEC_HEV_MISE*, *IEC_HEV_MIME* and *IEC_HEV_All*. The neural networks were trained to learn optimal solutions generated by DP based on these roadway types and congestion levels. .

- *IEC_HEV_SISE*. In this energy controller, for every R_i , two power split neural networks, $NN_{P_{bat}}^i$ and $NN_{\omega_{eng}}^i$ are trained with the data along the single optimal path generated by the DP optimization algorithm when it is applied to the FS drive cycle R_i , with the initial and the ending battery SOC set to 50%, $i=1, \dots, 11$. We refer this training method to as Single Initial point and Single Ending point (SISE), a single optimal path generated by DP that initiates at a single SOC point and ends at the same SOC point. Figure 7 (a) shows such an optimal SOC path generated the DP algorithm for the Sierra FS drive cycle Arterial LOS AB cycle (R_8). The optimal power split, optimal battery power and engine speed, along this optimal path were used as objective values for training the two neural networks, $NN_{P_{bat}}^i$ and $NN_{\omega_{eng}}^i$ where $i=8$.
- *IEC_HEV_MISE*. In this energy controller, the two power split neural networks for each roadway type and traffic congestion level R_i are trained with the data from the multiple optimal paths generated by the DP algorithm applied to the Sierra FS cycle represented by R_i . These multiple optimal paths are generated as follows. We apply the DP optimization algorithm to the FS drive cycle, R_i multiple times. At every time, the DP starts at a different initial battery SOC point but always ends at 50% of SOC. The optimal power split, optimal battery power and engine speed, along all these optimal paths were used as objective values for training the two power split neural networks. This training method is referred to as MISE (Multiple Initial SOC points and Single Ending SOC point). This training method is particularly feasible for real time vehicle energy management, where SOC is allowed to vary in the range of $[S_1, S_2]$. For the experiments presented in this paper, we use $S_1 = 0.4$ and $S_2 = 0.6$. For this reason, we used the DP algorithm to generate multiple optimal paths from the initial SOC points at 0.42, 0.46, 0.48, 0.5, 0.52, 0.54, 0.56, and 0.58. All paths end at 50% SOC. Figure 7 (b) shows the optimal paths generated from the Arterial LOS AB cycle (R_8). The same procedure is applied to every Sierra FS drive cycle for generating optimal power split points used to train the power split neural networks in *IEC_HEV_MISE*.
- *IEC_HEV_MIME*. In this energy controller, the two power split neural networks for each roadway type and traffic congestion level R_i are trained with the data from the multiple optimal paths generated by the DP algorithm from the FS drive cycle R_i with multiple initial battery SOC points and multiple ending SOC points. This training method is referred to as MIME (Multiple Initial SOC points and Multiple Ending SOC points). Similar to *IEC_HEV_MISE*, we assumed

an SOC operating range of $[S_1, S_2] = [0.4, 0.6]$. In this case, the DP algorithm generated multiple optimal paths from SOC starting points at 0.42, 0.46, 0.48, 0.5, 0.52, 0.54, 0.56, and 0.58. Each path ends with at the same SOC points as the initial SOC point, as illustrated in Figure 7 (c).

- *IEC_HEV_All*. In order to study the effectiveness of roadway type and traffic congestion level specific energy optimization, we trained the power split neural networks without making the distinction of roadway types and traffic congestion levels. The DP algorithm was applied to all 11 Sierra SF drive cycles with the initial and ending SOC set to 0.5. The resulting optimal power split points were used to train two power split neural networks, $NN_{P_{bat}}$ and $NN_{\omega_{eng}}$. During a real-time drive cycle, the *IEC_HEV_All* controller applies these two energy control neural networks to all roadway types and the traffic congestion levels. Figure 8 shows the configuration of *IEC_HEV_All*. The controller only has three neural networks, the neural network NN_DT trained for predicting driving trend, and the two power split neural networks, $NN_{P_{bat}}$ and $NN_{\omega_{eng}}$. $NN_{P_{bat}}$ and $NN_{\omega_{eng}}$ are used for all roadway types and traffic congestion levels to generate desired battery power demand and desire engine speed at every time instance t during real time vehicle operation.

The following subsections presents the experiments used to evaluate these systems.

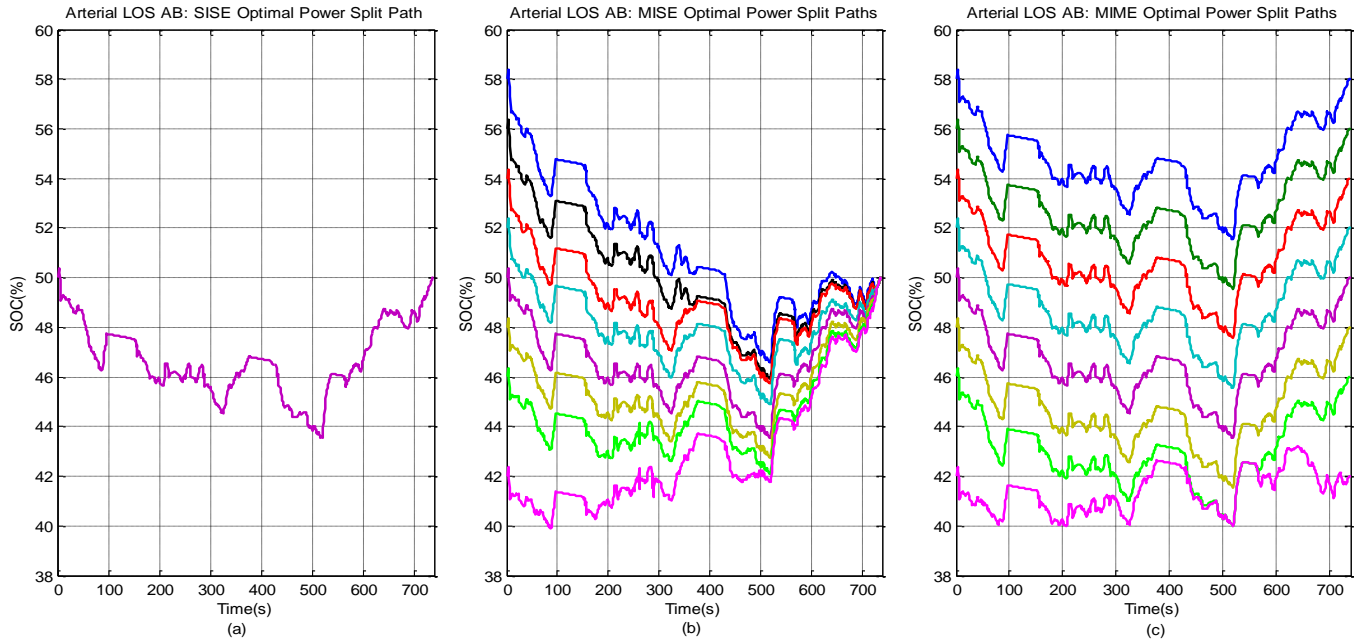


Figure 7. Optimal power split path generated from SF drive cycle Arterial LOS AB (a) Optimal energy path used in training IEC_HEV_SISE, (b) Optimal energy paths used in training IEC_HEV_MISE, (c) Optimal energy paths used in training IEC_HEV_MIME.

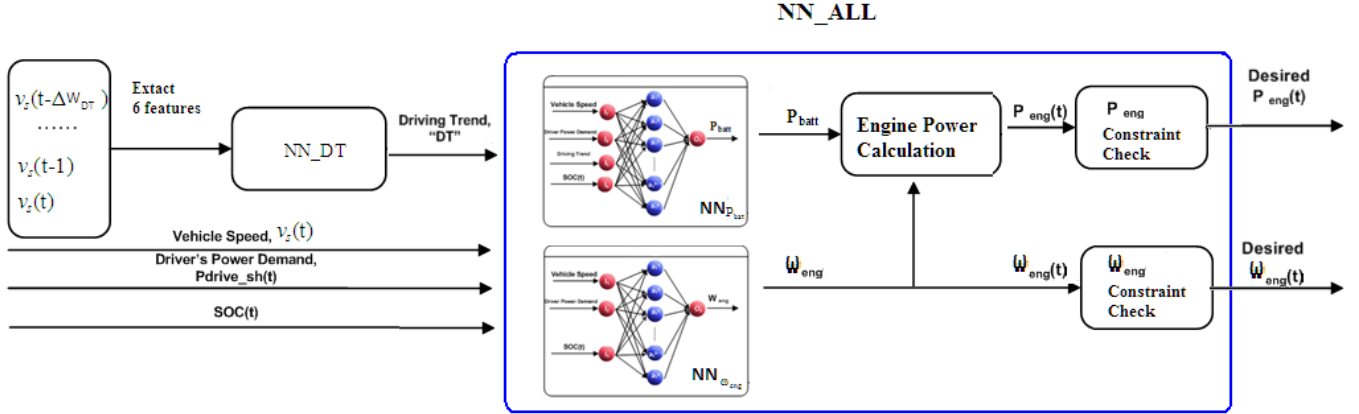


Figure 8. Energy control in *IEC_HEV_All*

A. Evaluation of *IEC_HEV*

In order to conduct an in-depth study of the power split control generated by proposed intelligent energy controller, we applied the *IEC_HEV_SISE* version to three drive cycles, LA92, NY_City, and Unif01. These three cycles are chosen because they represent well the real traffic conditions. Both LA 92 and Unif01 consist of combinations of freeway, arterial and local roads and various levels of traffic congestion levels. The NY_City is a typical city driving cycle with many brakes and a number of stop-and-go scenarios.

The study involves the analysis of the performances of *IEC_HEV* with respect to the accuracy of roadway type and traffic congestion level prediction, and the optimality of power split generated by *IEC_HEV* and represented in SOC, engine speed and battery power during the drive cycles, and fuel consumption over each drive cycle. The performances of *IEC_HEV* are compared with those generated by the Dynamic Programming (DP) through offline computation, which is often used in literature as the benchmark of the optimal performance, and those generated by the Ford Escape controller provided by PSAT system.

The results generated by the three systems over the three drive cycles are illustrated in Figures 9-11. Figures 9 - 11 (a) illustrate the roadway type and traffic congestion level prediction made by *IEC_HEV* over the three drive cycles. Each of those figures show the speed profile of the three cycles and the labeled true (in red color) and predicted (in blue color) roadway types and traffic congestion levels. The predictions were made every second ($\Delta t_n=1$) based on the features extracted from last 50 seconds of driving speed ($\Delta W_{RT} = 50$).

Figures 9 - 11(b) show the SOC changes during each of the three drive cycles generated by the three controllers, DP controller (in red color), *IEC_HEV_SISE* controller (in blue color), and the Ford Escape controller in PSAT (in green color), and Figures 9 -

11 (c) and (d) show the engine speed and battery power curves, respectively, generated by the three controllers. The SOC profile changes provide insight to how the controllers manage the battery power.

For the drive cycle LA 92, the SOC curve generated by the IEC_HEV_SISE was closer to the DP's SOC curve than the SOC curve generated by Ford Escape Default controller from $t=0$ through $t=400$ seconds. During $t=400$ seconds and $t=480$ seconds, the IEC_HEV_SISE controller was charging the battery, which causes the IEC_HEV_SISE's SOC increased 2.54% from the DP's SOC. Although this amount of deviation was carried through the remaining entire drive, the IEC_HEV_SISE's SOC still closely followed the trend of DP's SOC curve. From $t=1000$ through the end, the SOC curve generated by the Ford Escape Default controller behaved quite irregularly in comparison with the SOC curve generated by DP, while the SOC curve generated by the IEC_HEV_SISE still closely followed the trend of DP's SOC curve to the end. The ending SOC generated by IEC_HEV_SISE was equal to the starting point, which is 50%, while the ending SOC generated by the Ford Default Controller dropped below 47%. For the NY_City drive cycle and Unif01 cycle, the IEC_HEV_SISE followed the DP's SOC curve much closer than the default Ford Escape controller.

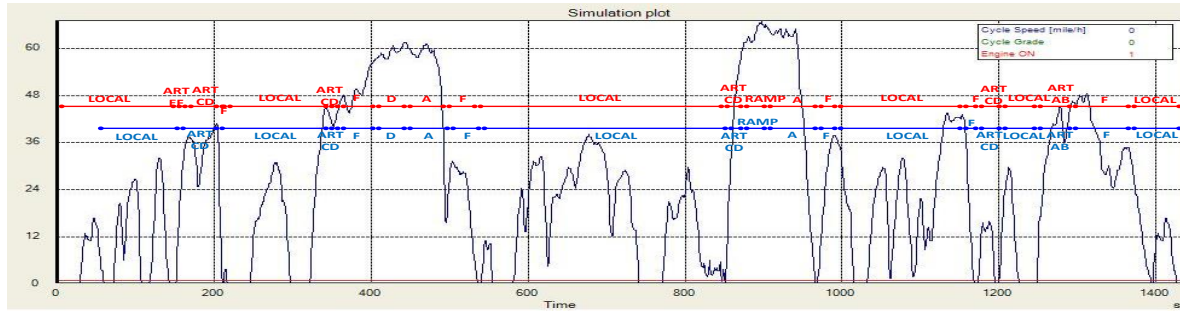
Tables II, III, and IV show the fuel savings by Dynamic Programming and the IEC_HEV_SISE controller in comparison with the default Ford Escape controller for LA92, NY_City, and Unif01 cycles, respectively. All experiments started with battery SOC set to 50%. However only the DP controller ended at 50% of SOC. In order to conduct a fair comparison, we adjust the fuel consumption based on the ending SOC using the following formula,

$$Adjusted\ fuel\ Cost = \left\{ \sum_{t=1}^N fuel\ rate(t) \right\} + \lambda(SOC(N) - SOC_{DP}(N)), \quad (7)$$

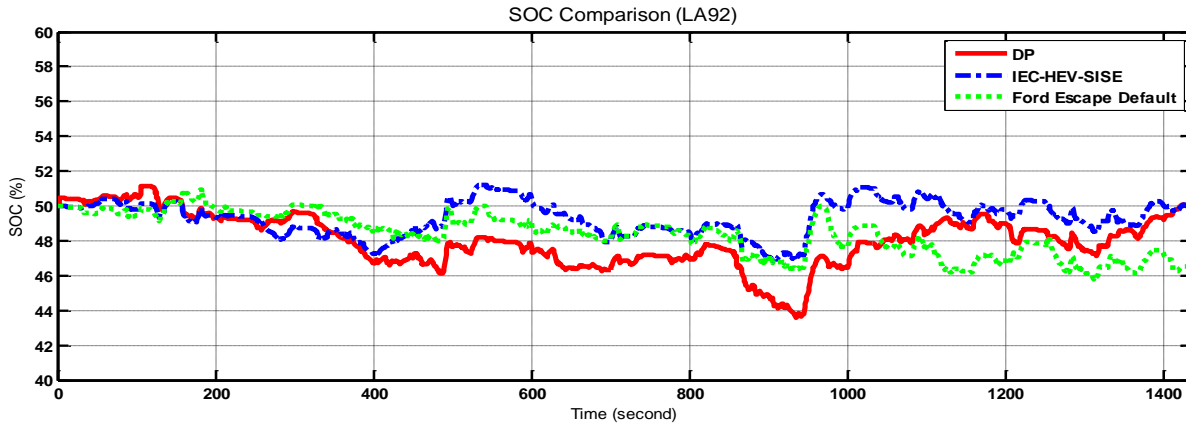
where $t=N$ is the end of a cycle, SOC_{DP} is a SOC generated by DP and λ is a fuel cost that is equivalent to 1 % of SOC. The value of λ is determined by running DP on the same drive cycle two times, each ends at a different SOC. For the drive cycle LA92, IEC_HEV_SISE saved over 9% fuel, for NY_City over 11% and Unif01 over 8%.

B. Evaluation of four different version of IEC_HEV

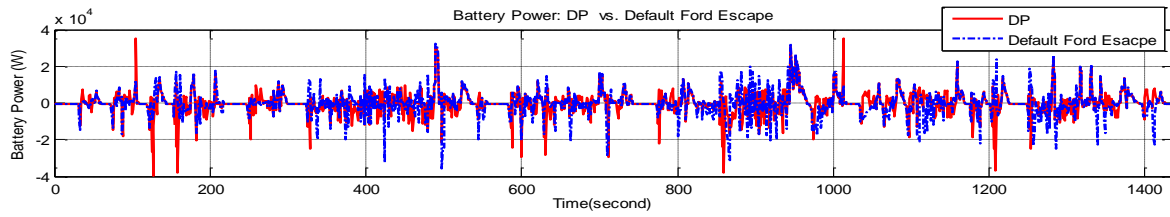
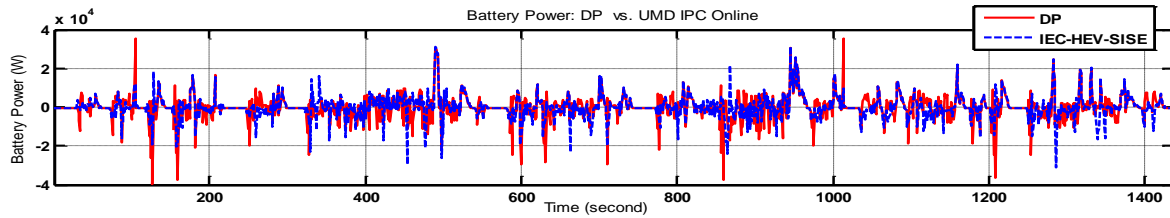
The three of the four versions of IEC_HEV controllers, IEC_HEV_SISE, IEC_HEV_MISE, IEC_HEV_MIME, are designed to evaluate the effectiveness of the optimal paths generated by the DP at various starting and ending SOC at the 11 Sierra FS drive cycles. The fourth controller, IEC_HEV_All, is designed to evaluate the effectiveness of roadway type and traffic congestion level specific power split. The evaluation of these four controllers are conducted based on their performances on the ten test drive cycles provided by the PSAT library, UDDS, SC03, HWFET, Arb02, NY_City, Rep05, LA92, HL07, US06, and Unif01. Figure 12 illustrates the fuel savings of the four controllers along with DP, the optimal controller, on all ten test drive cycles.



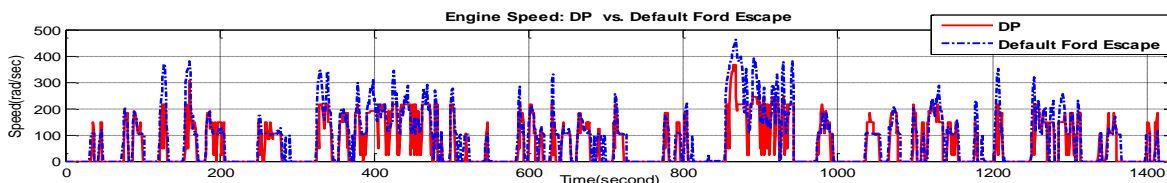
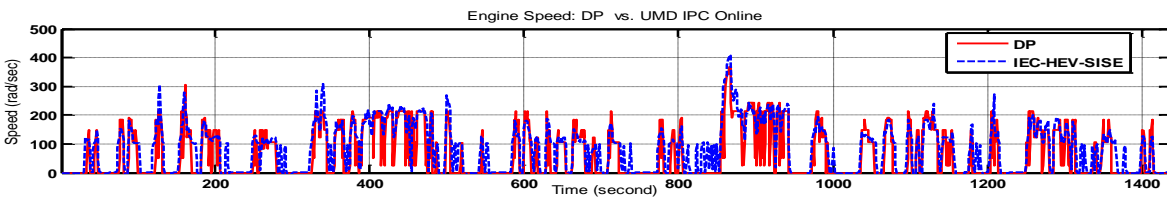
(a)



(b)



(c)



(d)

Figure 9. (a) Drive cycle LA92 labeled with true and predicted roadway types and traffic congestion levels; (b) SOCs of LA92 generated by the three controllers; (c) Engine speed ; (d) Battery power comparison;

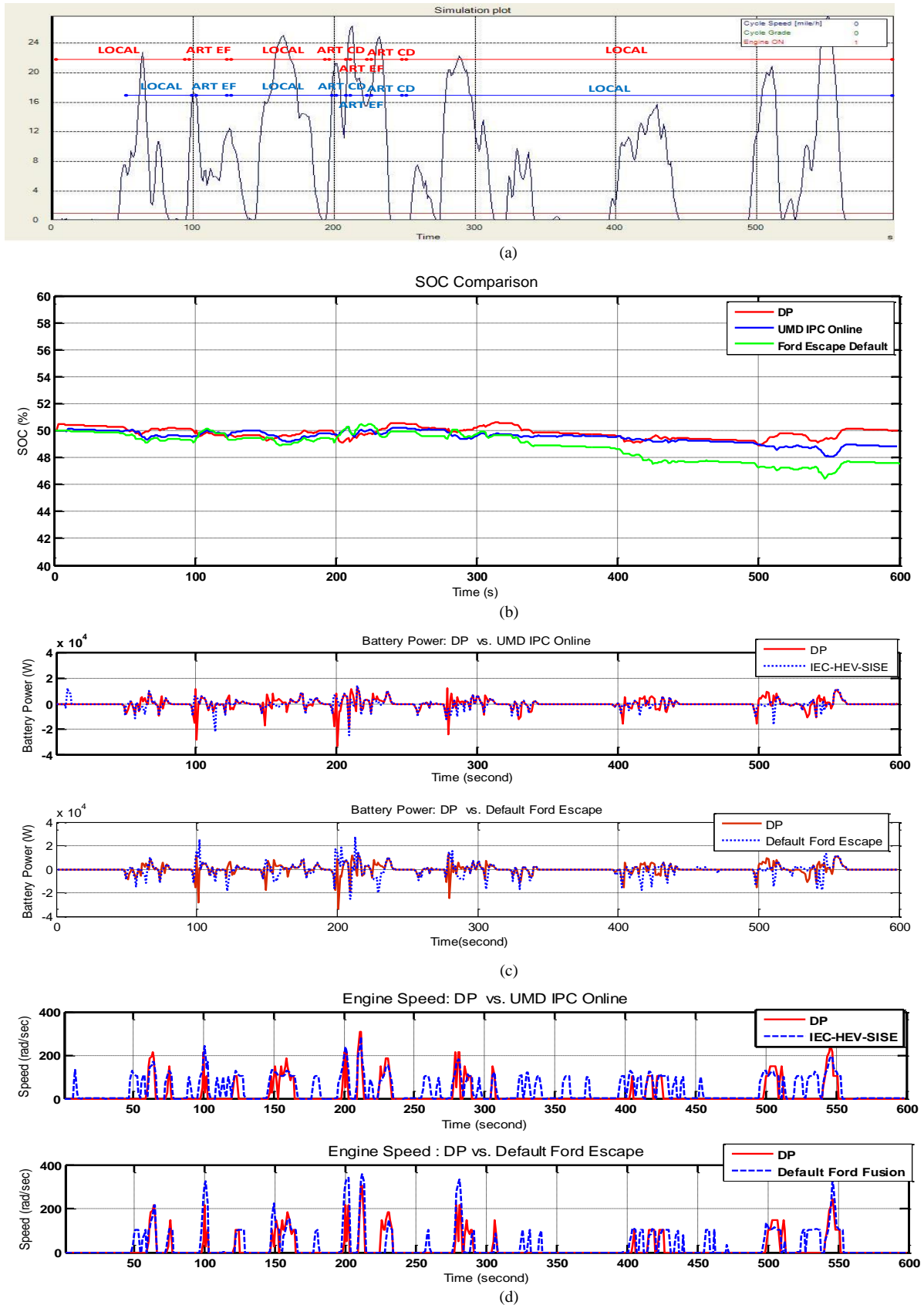
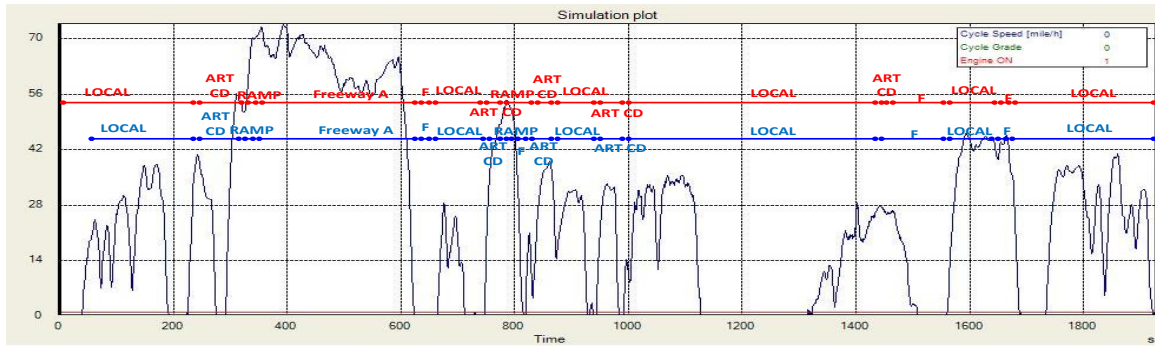
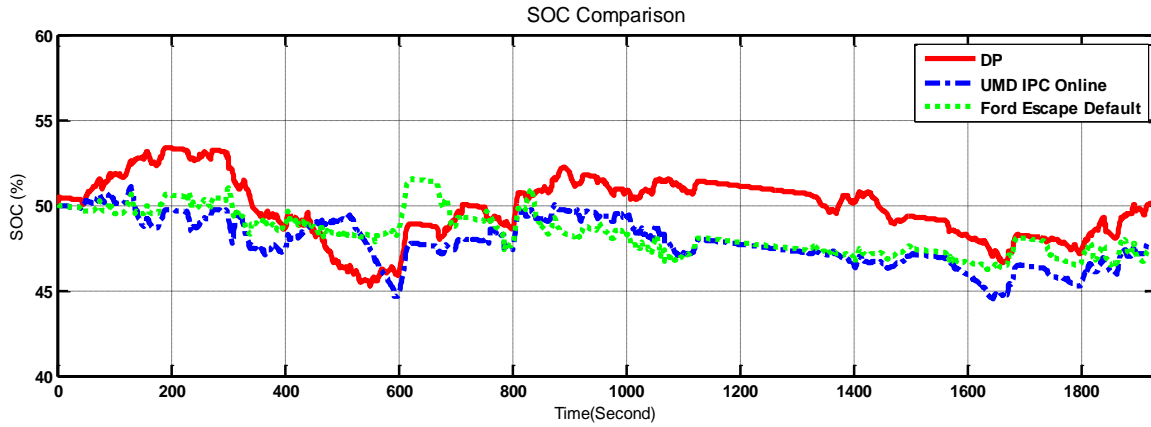


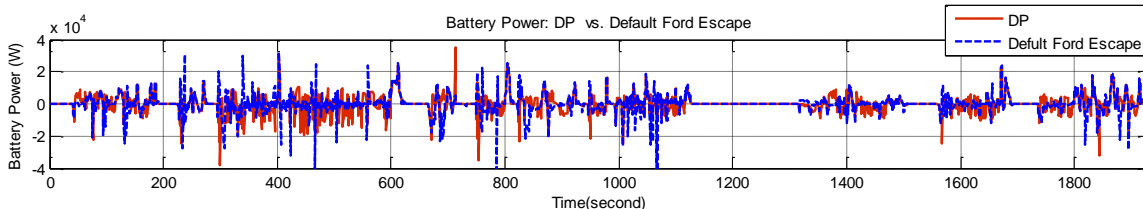
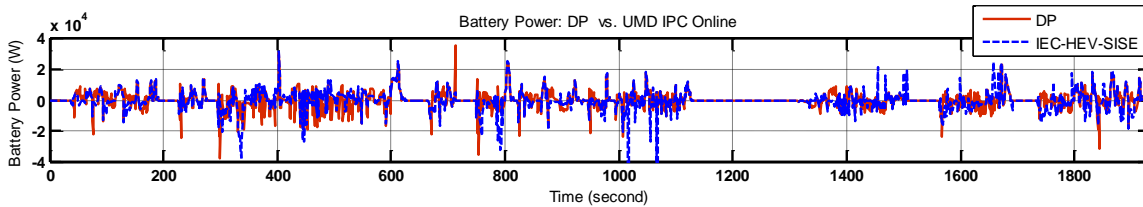
Figure 10. (a) Drive cycle NY_City labeled with true and predicted roadway types and traffic congestion levels; (b)SOCs of NY_City generated by the three controllers; (c) Engine speed ; (d) Battery power comparison.



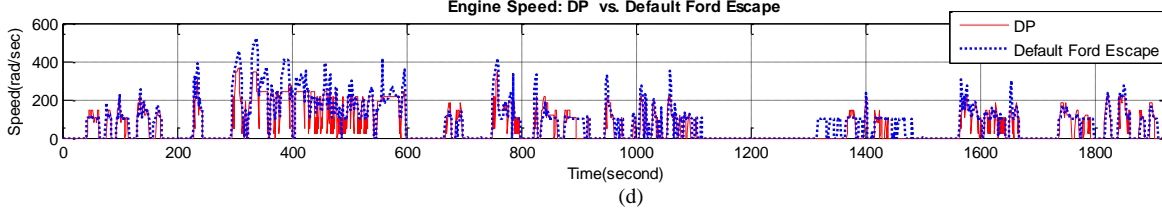
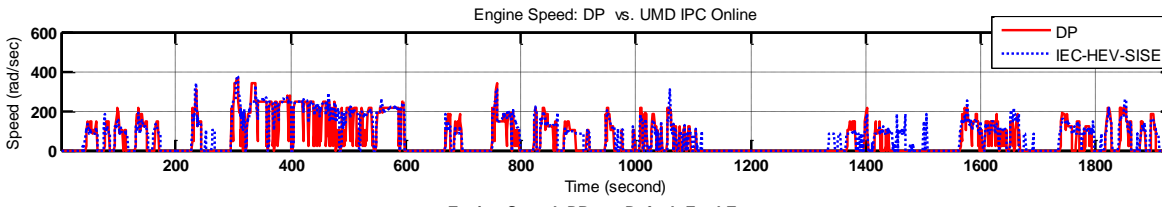
(a)



(b)



(c)



(d)

Figure 11. (a) Drive cycle Unif01 labeled with true and predicted roadway types and traffic congestion levels; (b)SOC comparison with Unif01; (c) Engine speed output comparison; (d) Battery power comparison.

TABLE II
FUEL SAVING FOR LA92

LA92	Fuel consumption before SOC correction (g)	Ending SOC (%)	Fuel consumption after SOC correction (g)	Saving (%)
PSAT	898.90	46.51	916.36	
DP	754.65	50.00	754.65	17.65%
IEC_HEV_SISE	830.94	50.00	830.94	9.32%

TABLE III
FUEL SAVING FOR NY_City

NY_City	Fuel consumption before SOC correction (g)	Ending SOC (%)	Fuel consumption after SOC correction (g)	Saving (%)
PSAT	125.49	47.57	137.65	
DP	108.84	50.00	108.84	20.93%
IEC_HEV_SISE	117.42	48.81	123.35	11.16%

TABLE IV
FUEL SAVING FOR Unif01

Unif01	Fuel consumption before SOC correction (g)	Ending SOC (%)	Fuel consumption after SOC correction (g)	Saving (%)
PSAT	1198.221	47.23	1212.085	
DP	1013.148	50.00	1013.148	16.41%
IEC_HEV_SISE	1075.642	47.88	1113.307	8.15%

Dynamic Programming cannot be used for in-vehicle control since it requires a priori knowledge of the entire drive cycle and is too computationally intensive to be done in real-time. Furthermore, in production systems such as the Ford Escape or Toyota Prius, other factors such as drivability, performance, and emissions need to be balanced with vehicle energy management. For this reason, DP only serves as an upper bound of energy optimization in a vehicle for a given drive cycle.

It appears that *IEC_HEV_MISE* controller has the best performances. It outperformed *IEC_HEV_SISE* on 8 drive cycles. It outperformed *IEC_HEV_MIME* on 5 drive cycles, and has equal or close performances on two drive cycles (Rep05 and NY_City). For the remaining three drive cycles, SC03, HWFET and Arb02, *IEC_HEV_MISE* is only slightly behind *IEC_HEV_MIME*. In comparison with *IEC_HEV_All*, *IEC_HEV_MISE* has large leads over *IEC_HEV_All* on all drive cycles except on LA92, on which, *IEC_HEV_MISE* has similar fuel saving as *IEC_HEV_All*. In summary, *IEC_HEV_MISE* has the best fuel savings over all test drive cycles.

Figure 13 shows the ending SOC for each of the simulations. The ending SOC of *IEC_HEV_SISE* in all ten test drive cycles stayed most close to the beginning SOC, which is 50% in comparison with the other three controllers. *IEC_HEV_MISE* comes in the second place in terms of closeness to the beginning SOC over all test drive cycles. The *IEC_HEV_MIME* controller generated large swings in ending SOC. In most test drive cycles, *IEC_HEV_All* ended at low SOC.

If fuel savings and battery management are considered together, we can conclude that *IEC_HEV_MISE* is the best controller, and *IEC_HEV_SISE* is the second best. Because of the inferior performances of *IEC_HEV_All* in terms of both fuel saving and battery management, we can further conclude that machine learning of optimal power split based on roadway types and traffic congestion levels is an effective approach of intelligent energy management in vehicle.

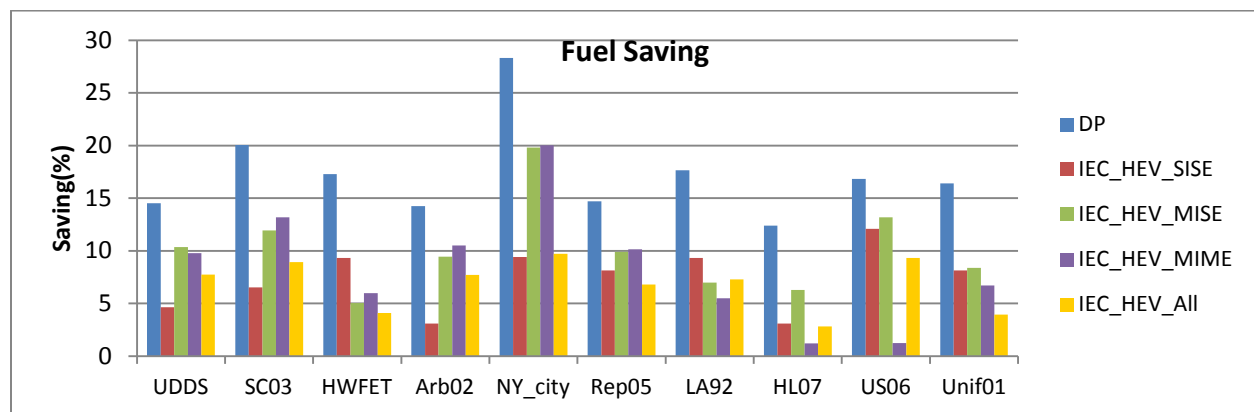


Figure 12. Comparisons of fuel savings by Dynamic programming and *IEC-HEV* controllers.

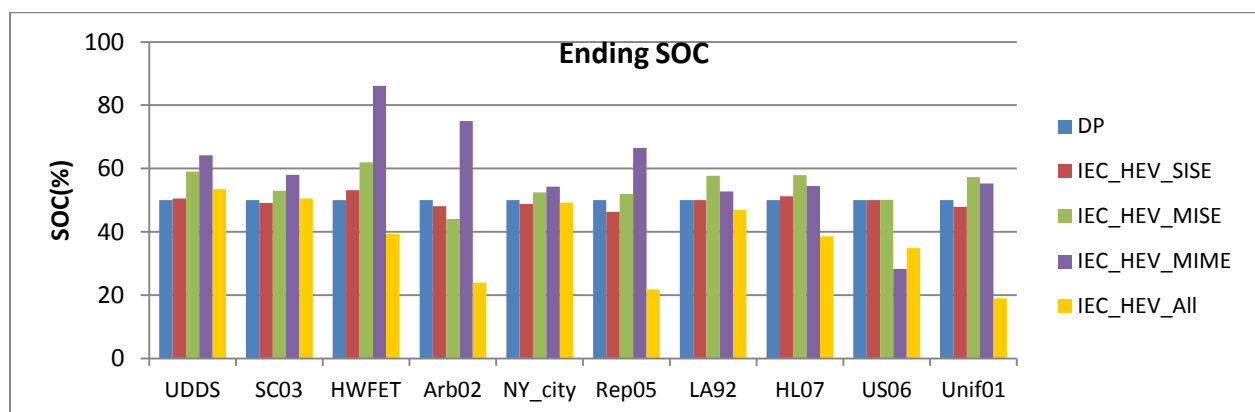


Figure 13. Comparisons of ending SOC over all test drive cycles.

IV. Conclusion

The choice of the power split during the "engine on" mode is the most important opportunity in the vehicle power controller for optimizing fuel economy. Our major contribution is to provide intelligent online energy control while the vehicle is operating in the power split mode. We developed and implemented three intelligent energy controllers under the proposed machine learning framework, *ML_EMO_HEV*, which combines Dynamic Programming with machine learning to learn about roadway type and traffic congestion level specific optimal power split during the "engine on" mode. The details of *ML_EMO_HEV* can be found in the Part I of the series. All three online controllers, *IEC_HEV_SISE*, *IEC_HEV_MISE*, and *IEC_HEV_MIME*, consist of three major types of neural networks, a neural network trained to predict roadway types and traffic congestion levels, a driving trend prediction neural network, and 22 power split neural networks trained specifically for the 11 roadway types and traffic congestion levels defined by Sierra Research. The output from the power split neural networks are optimal engine speed, $\omega_{eng}(t)$, and optimal battery power, $P_{batt}(t)$, which are then used to generate the optimal engine power, $P_{eng}(t)$. In turn, both $P_{eng}(t)$ and $\omega_{eng}(t)$ are checked to make sure they are within the appropriate constraints.

The three *IEC_HEV* controllers have been implemented inside the Ford Escape model in PSAT for performance evaluations. Their performances on the 10 test drive cycles provided by PSAT are analyzed and compared with the DP offline optimal controller and the default controller used in the Ford Escape model provided by PSAT. We also evaluated the effectiveness of roadway type and traffic congestion level specific power split by comparing the performances of the three controllers with *IEC_HEV_All*, an *IEC_HEV* controller containing two power split neural networks applicable to all roadway types and traffic congestion levels. Based on these experiments, we can make the following conclusions.

- The *IEC_HEV* controllers trained with the proposed machine learning framework, including the *IEC_HEV_All*, provide substantial savings on all drive cycles. The fuel savings range from 3%~20% over the default Ford Escape model for the ten PSAT cycles.
- The roadway type and traffic congestion level specific trained *IEC_HEV* controllers, *IEC_HEV_SISE*, *IEC_HEV_MISE*, and *IEC_HEV_MIME*, in general have better performance than the general *IEC* controller, *IEC_HEV_All*.
- The best controller is *IEC_HEV_MISE*. It is a roadway type and traffic congestion level specific intelligent energy controller trained with multiple optimal paths generated by DP with multiple initial SOC points and the one ending SOC at 50%. This controller provides substantial fuel savings and stable SOC control in all drive cycles.

ACKNOWLEDGMENT

This work was supported in part by a grant from the State of Michigan under the 21st Jobs Fund, a grant from the Ford Alliance Program, and a grant from the Institute of Advanced Vehicle Systems at the University of Michigan-Dearborn

REFERENCES

- [1] K Wipke, T Markel, and D Nelson, "Optimizing Energy Management Strategy and Degree of Hybridization for a Hydrogen Fuel Cell SUV," *Proceedings of 18th International Electric Vehicle Symposium (EVS 18)*, Berlin, 2001.
- [2] S. Jeon, S. Jo, Y. Park, J. Lee, "Multi-Mode Driving Control of a Parallel Hybrid Electric Vehicle Using Driving Pattern Recognition," *ASME Journal of Dynamic Systems, Measurement, and Control*, Vol. 124, No. 1, pp. 141-149, 2002.
- [3] Y. Zhu, Y. Chen, Z. Wu, A. Wang, "Optimization design of an energy management strategy for hybrid vehicles," *International Journal of Alternative Propulsion 2006 - Vol. 1, No.1* pp. 47 - 62.
- [4] Y. Zhu, Y. Chen, and Q. Chen, "Analysis and Design of an Optimal Energy Management and Control System for Hybrid Electric Vehicles," *Proc. of the 19th Electric Vehicles Symposium*, Busan, Korea, 2002.
- [5] N. Schouten, M. Salman, N. Kheir, "Fuzzy Logic Control for Parallel Hybrid Vehicles," *IEEE Transactions on Control Systems Technology*, Vol. 10, No. 3, pp.460-468, 2002.
- [6] E. D. Tate and S. P. Boyd, "Finding ultimate limits of performance for hybrid electric vehicles," *Society of Automotive Engineers Paper-01-3099*, 2000.
- [7] S. Delprat, J. Lauber, T.M. Guerra, and J. Rimaux, "Control of a parallel hybrid powertrain: optimal control," *IEEE Transactions on Vehicular Technology*, vol. 53, no. 3, pp. 872-881, May 2004.
- [8] C.-C. Lin, H. Peng, J.W. Grizzle, and J.-M. Kang, "Power management strategy for a parallel hybrid electric truck," *IEEE Transactions on Control System Technology*, vol. 11, no. 6, pp. 839-849, Nov. 2003.
- [9] T. Hofman and R. van Druen, "Energy analysis of hybrid vehicle powertrains," in *Proc. IEEE Int. Symp. Veh. Power Propulsion*, Paris, France, Oct. 2004.
- [10] I. Arsie, M. Graziosi, C. Pianese, G. Rizzo, and M. Sorrentino, "Optimization of supervisory control strategy for parallel hybrid vehicle with provisional load estimate," in *Proc. 7th Int. Symp. Adv. Vehicle Control (AVEC)*, Arnhem, the Netherlands, Aug. 2004.
- [11] T. R. Carlson and R. C. Austin, "Development of speed correction cycles," Sierra Research, Inc., Sacramento, CA, Report SR97-04-01, 1997.
- [12] Sierra Research, "SCF Improvement – Cycle Development," Sierra Report No. SR2003-06-02, 2003.
- [13] Langari, R.; Jong-Seob Won, "Intelligent energy management agent for a parallel hybrid vehicle-part I: system architecture and design of the driving situation identification process," *IEEE Transactions on Vehicular Technology*, vol. 54, issue 3, pp. 925 – 934, 2005.
- [14] Jong-Seob Won; Langari, R., "Intelligent energy management agent for a parallel hybrid vehicle-part II: torque distribution, charge sustenance strategies, and performance results," *IEEE Transactions on Vehicular Technology*, vol. 54, issue 3, pp. 935 – 953, 2005.
- [15] Jungme Park, ZhiHang Chen, Leonidas Kiliaris, Ming Kuang, Abul Masrur, Anthony Phillips and Yi L. Murphey, "Intelligent Vehicle Power Control based on Machine Learning of Optimal Control Parameters and Prediction of Road Type and Traffic Congestions," *IEEE Transactions on Vehicular Technology*, Vol 58, No. 9, November, 2009.
- [16] F.U. Syed et al., "Derivation and Experimental Validation of a Power-Split Hybrid Electric Vehicle Model," *IEEE Transactions on Vehicular Technology*, vol. 55, 2006, p. 1731.
- [17] M. Kuang, D. Hrovat, "Hybrid Electric Vehicle Powertrain Modeling and Validation", *Proc. of EVS 14, the 20th International Electric Vehicle Symposium and Exposition*, Nov., 2003.

- [18] A. M. Phillips, M. Jankovic, and K.E. Bailey, "Vehicle system controller design for a hybrid electric vehicle," Proceedings of the 2000 IEEE International Conference on Control Applications, 2000
- [19] J. T. B. A. Kessels," Energy Management for Automotive Power," Dissertation, Mechanical engineering, Technische Universiteit Eindhoven, 2007.
- [20] C.-C. Lin, H. Peng, and J.W. Grizzle, "A stochastic control strategy for hybrid electric vehicles," in Proc. Amer. Contr. Conf., Boston, MI, Jun. 2004, pp. 4710–4715.
- [21] Jungme Park, Zhihang Chen and Yi Murphey , "Intelligent Vehicle Power Management through Neural Learning," International Joint Conference on Neural Networks, July 2010.
- [22] Yi L. Murphey, Jungme Park, ZhiHang Chen, Ming Kuang, Abul Masrur, Anthony Phillips, "Intelligent Hybrid Vehicle Power Control - Part I: Machine Learning of Optimal Vehicle Power," Submitted to IEEE Transaction on Vehicular Technology, September 2011.